THE JOURNAL OF PHYSICAL CHEMISTRY B

Article

pubs.acs.org/JPCB

Structure Dependence of Charged States in "Linear" Polyaniline as Studied by In Situ ATR-FTIR Spectroelectrochemistry

Andrea Kellenberger,*[,†,‡] Evgenia Dmitrieva,[†] and Lothar Dunsch*[,†]

[†]Center of Spectroelectrochemistry, Department of Electrochemistry and Conducting Polymers, Leibniz Institute for Solid State and Materials Research, IFW Dresden, Helmholtzstrasse 20, D-01069 Dresden, Germany

[‡]Faculty of Industrial Chemistry and Environmental Engineering, University "Politehnica" of Timisoara, Piata Victoriei 2, RO-300006 Timisoara, Romania

ABSTRACT: The electrochemical doping of emeraldine salt and emeraldine bases with different weight average molecular weights was studied by in situ Fourier transform infrared (FTIR) spectroelectrochemistry using attenuated total reflection (ATR) technique. The formation and stabilization of charge carriers in polyaniline during p-doping was followed in dependence of the chain branching. The potential dependence of the IR bands during the oxidation of the polymer clearly demonstrates the formation of the different charged polymer structures (π-dimers, polarons, and bipolarons). It is shown that IR bands usually attributed to a semiquinoid polaron lattice correspond in fact to doubly charged species, π-dimers, which are face-to-face complexes of two polarons. Bands corresponding exclusively to polarons have been identified at 1266, 1033, and 1010 cm^{-1}, suggesting that polarons are predominantly stabilized on the linear segments near the polymer branches by phenazine.

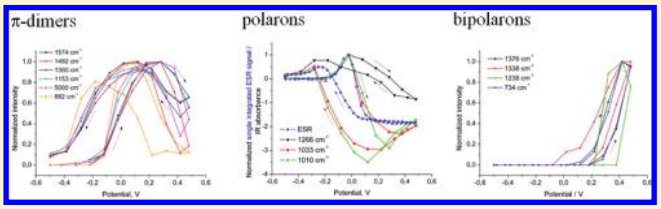

INTRODUCTION

The chemical structure of polyaniline (PANI) is often given by a linear model with three oxidation states of the polymer: the completely reduced leucoemeraldine, the intermediate emeraldine, and the fully oxidized pernigraniline base.[1] Switching between the different oxidation states of PANI can be realized by chemical or electrochemical doping/dedoping. In a typical cyclic voltammogram of PANI, the first redox peak has been attributed to the transformation of leucoemeraldine into emeraldine, and the second main peak to the further oxidation of emeraldine to fully oxidized pernigraniline form.[2] Considering a linear PANI structure, the well-accepted polaron−bipolaron model for conducting polymers is interpreted as follows: the polaron (radical cation) is the singly oxidized form of a polymer segment with spin $s = 1/2$ and two optical transitions; the bipolaron (dication) is a doubly oxidized form, which is diamagnetic and has one optical transition.[3,4] Miller and co-workers suggested a *polaron-π-dimer model* in addition to bipolarons in oxidized polythiophene.[5] The π-dimer is considered as a face-to-face complex of two radical cations interacting through their π-orbitals. However, π-dimers formed during p-doping of conducting polymers are also reported for polypyrole[6] or PANI.[7] Our group has previously shown that the most important intermediate formed during aniline polymerization, the p-aminodiphenylamine, forms a π-dimer of two radical cations under oxidation in acidified organic solvents.[8]

Fourier transform infrared (FTIR) spectroscopy as a powerful tool for identifying types of chemical bonds in a molecule by the molecular "fingerprint" is used in combination with electrochemistry for detailed structural information on the intermediates and products in a charge transfer reaction. Attenuated total reflection (ATR) technique is especially useful for IR measurements of solids (films, polymers and powders), semisolids (pastes, creams, gels), and liquids as well as dark colored materials. By in situ ATR-FTIR spectroelectrochemistry, structural changes in the polymer film during its doping can be followed.[9−11]

During the first oxidation peak of electrochemically prepared PANI, the IR bands at 1564, 1481, 1304, 1250, and 1144 cm^{-1} were attributed to a semiquinoid polaron lattice structure.[12,13] The second oxidation step results in the formation of quinoid structures with vibrations at 1625, 1569, 1376, 1341, and 846 cm^{-1}. The IR band at 1250 cm^{-1} is often attributed to the polaron lattice structure[14] based on its analogy in Raman spectroscopic studies, giving a Raman band at around 1253 cm^{-1} attributed to the C−$N^{\bullet+}$ stretching mode in the semiquinone radical cations.[15,16] The broad absorption band centered at about 5000 cm^{-1} was interpreted as the intermediate oxidized metallic form of PANI.[17,18] Most studies on the electronic structure of PANI have used the linear structure model for interpretations in which PANI consists of a linear arrangement of the monomers. However, early works have shown that phenazine rings have to be considered as a part of the polymer chain for both chemically and electrochemically prepared PANI.[19−23] Such branches occur by aniline coupling reaction in the ortho-position of the quinoid structures - a reaction well-known in organic chemistry. The following intramolecular cyclization results in the formation of

Received: December 2, 2011
Revised: March 11, 2012
Published: March 12, 2012

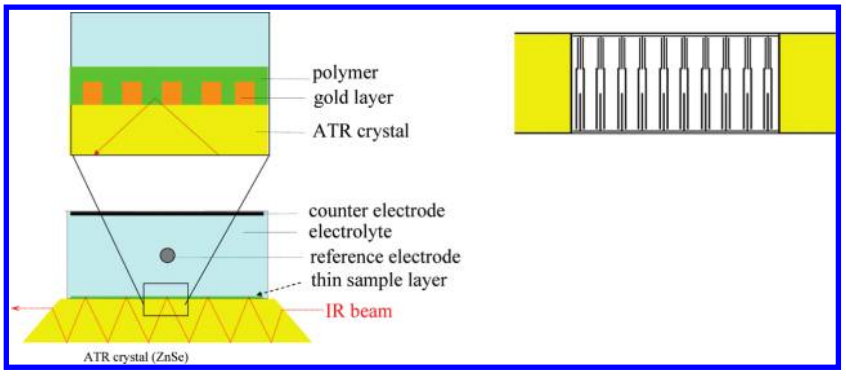

Figure 1. Schematic representation of the spectroelectrochemical cell (left) and of the ATR crystal covered with a gold conducting layer (right - top view) used for in situ ATR-FTIR spectroelectrochemistry.

phenazine rings. Therefore, the linear structure of the PANI is an idealized structure model and does not represent the real polymer structure.

It has been shown by FTIR spectroscopy that branching of the polymer chain as well as small amounts of phenazine units are present in commercially available emeraldines as a

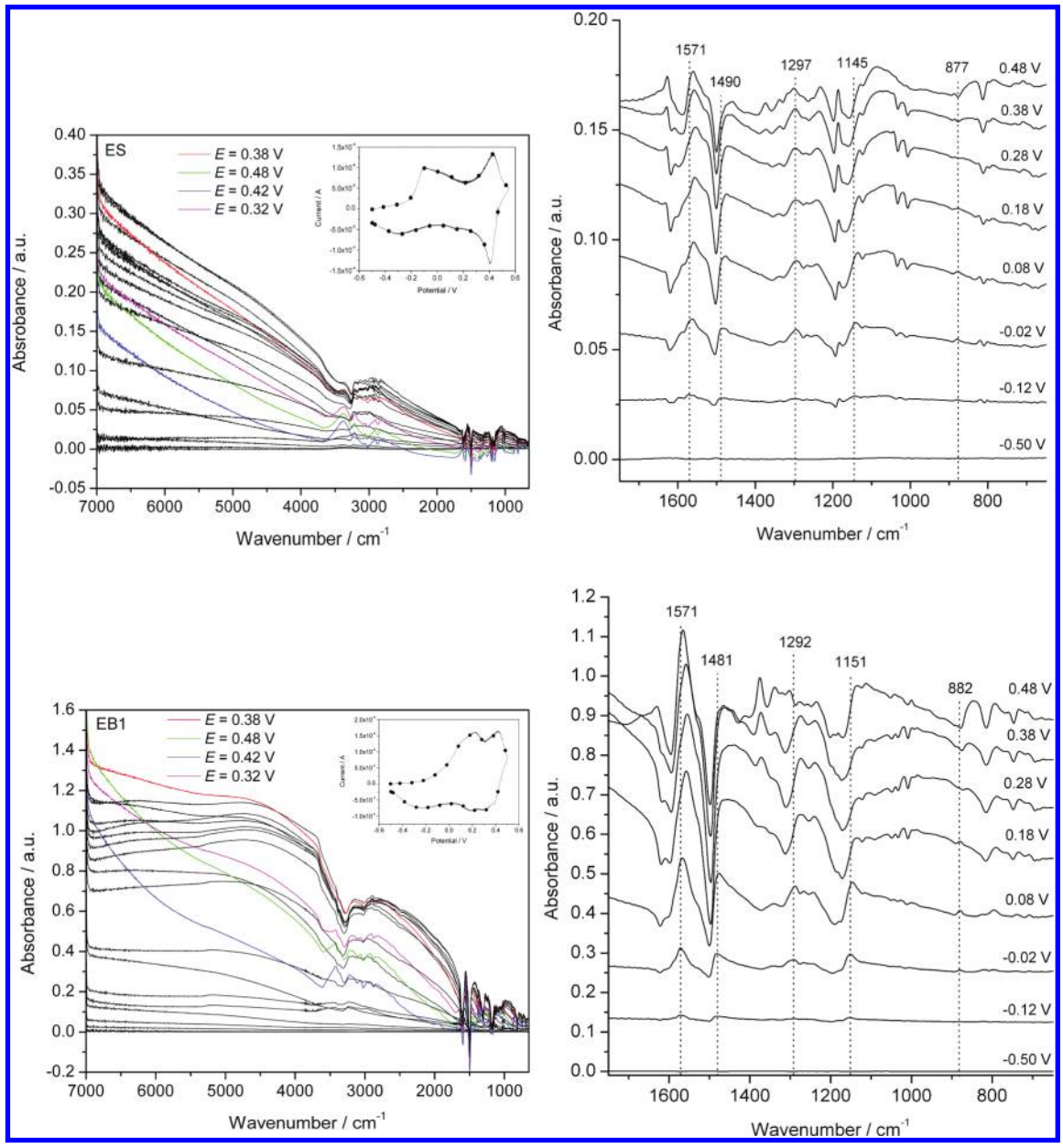

Figure 2. continued

dx.doi.org/10.1021/jp211595n | J. Phys. Chem. B 2012, 116, 4377–4385

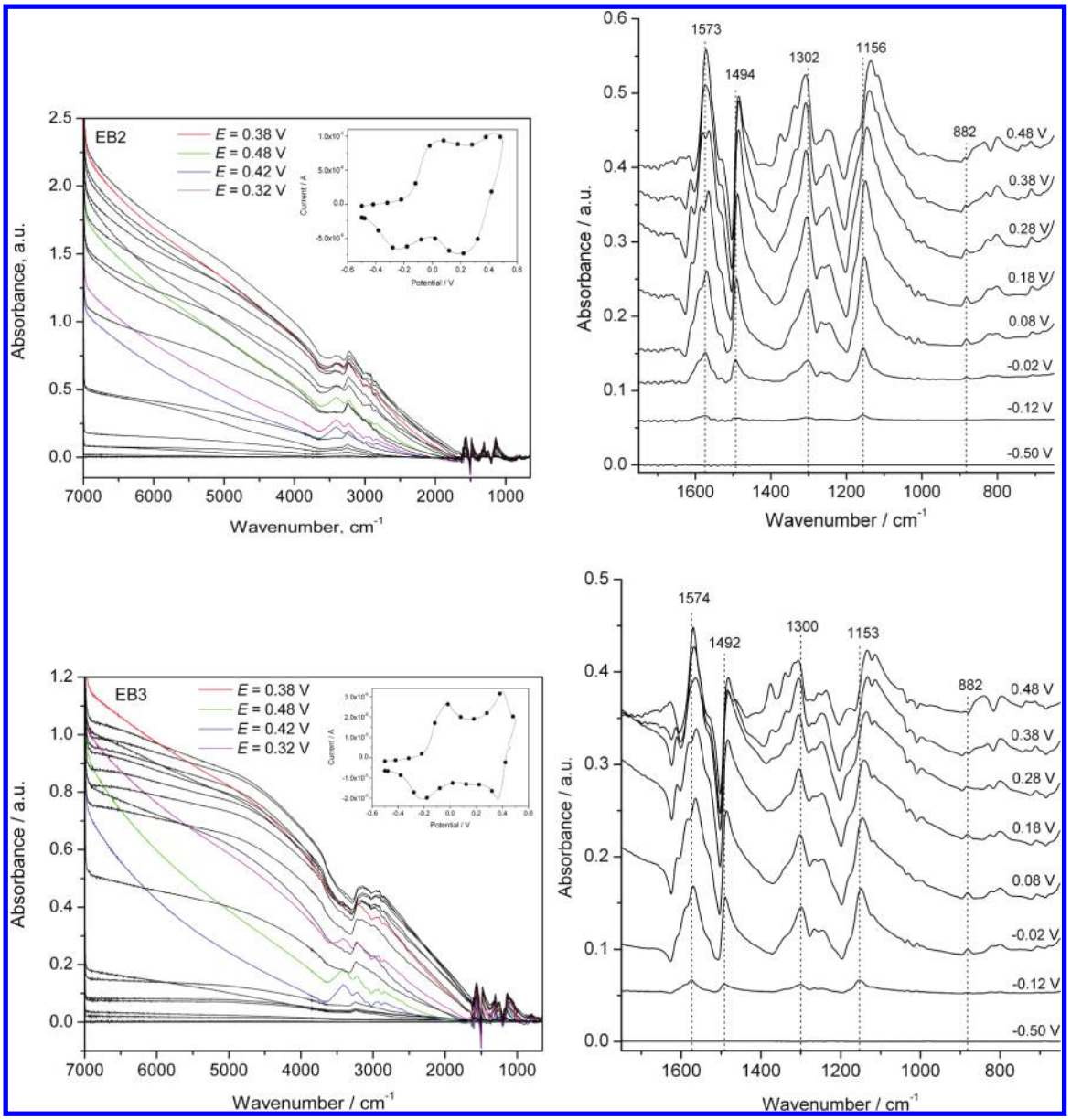

Figure 2. In situ ATR-FTIR spectra of different PANI structures upon charging. Left: wavenumber range 7000−650 cm^{-1} and simultaneous cyclic voltammograms for ES, EB1, EB2 and EB3 (insert, triggers are marked with points). Right: Enlarged in situ ATR-FTIR spectra in the wavenumber range 1750−650 cm^{-1} for the corresponding polymer structures. Spectra are deconvoluted.

powder.[24] The branching of the polymer chains increases with the increasing of the weight average molecular weight of emeraldines. The aim of this paper was to investigate the structure dependence of the formation of charge carriers in so-called "linear" emeraldines during p-doping by means of in situ ATR-FTIR spectroelectrochemistry pointing to the role of phenazine structure in the stabilization of charged states.

■ EXPERIMENTAL SECTION

Commercially available emeraldine bases with different weight average molecular weights (average $M_w \approx 5000$, 50 000, and 300 000, Aldrich) and emeraldine salt (average $M_w > 15\,000$, Aldrich) are denoted as EB1, EB2, EB3, and ES, respectively.

The FTIR measurements are performed with the ATR technique, using a VERTEX 80v (Bruker Optics, Germany) spectrometer equipped with a liquid nitrogen-cooled mercury cadmium telluride (MCT) detector. Each FTIR spectrum results from 100 scans with a resolution of 4 cm^{-1}. The in situ FTIR spectroelectrochemical measurements are controlled by a PG 390 potentiostat/galvanostat (HEKA Electronic, Lambrecht, Germany) equipped with the PotMaster v2 × 52 software that triggers the FTIR spectrometer. To ensure a reasonable conductivity, the zinc selenide (ZnSe) internal reflection element used as the working electrode was covered with a fine gold interdigitated structure with a thickness of 50 nm deposited by photolithography. An intermediate chromium layer with a thickness of 5 nm is used to improve the gold layer adhesion. The ZnSe reflection element covered with the polymer film was mounted in the in situ spectroelectrochemical cell which was then filled with electrolyte solution. The in situ ATR-FTIR measurements are performed in a three-electrode arrangement in the spectroelectrochemical flow-through cell made of Teflon. A silver chloride-coated silver wire with a thin

dx.doi.org/10.1021/jp211595n | J. Phys. Chem. B 2012, 116, 4377−4385

Table 1. Analysis of the Peaks of In Situ FTIR Spectra of Different PANI Structures in the Mid-infrared Region

EB1	EB2	EB3	ES	assignment[a]
1571	1573	1574	1571	ring stretching in SQ (↑ up to 0.3 V then ↓)
1481	1494	1492	1490	ring stretching in SQ (↑ up to 0.3 V then ↓)
1292	1302	1300	1297	ν (C−N) in SQ ring (↑ up to 0.3 V then ↓)
1151	1156	1153	1145	δ (C−H) in SQ or ν (HSO_4^-) (↑ up to 0.3 V then ↓)
882	882	882	878	γ (C−H) in 1,2,4-trisubstit B ring (2-substit phenazine ring) (↑ up to 0.3 V then ↓)
1598	1605	1604	1600	ν (C−C) in Q ring (↓ in the forward scan)
1502	1507	1506	1505	ν (C−C) in B ring (↓ in the forward scan)
1197	1197	1196	1193	ν (C−N) in aromatic amine (↓ in the forward scan)
814	818	816	810	γ (C−H) in 1,4 substit B ring (↓ in the forward scan)

[a]Assignments are based on refs 13−17 and 25−34. ν, stretching mode; δ, in-plane bending mode; γ, out-of-plane bending mode; B, benzene ring; Q, quinoid ring; SQ, semiquinoid structure. ↑ increasing peak intensity; ↓ decreasing peak intensity.

flexible Teflon insulation serves as a pseudoreference electrode, and a platinum foil serves as a counter electrode.

The polymers were dissolved in dimethyl sulfoxide (DMSO; puriss., Aldrich) and deposited on an ATR crystal by drop coating, followed by solvent evaporation under nitrogen flow. The solubility of the polymers in DMSO decreases with increasing weight average molecular weight. The spectroelectrochemical investigations of the polymers were carried out in aqueous solution of 0.1 M sulphuric acid (Merck, 95−97%) and 0.01 M sodium *p*-toluenesulfonate (Merck, 98%) as a surfactant agent to minimize the degradation rate of the polymer films during the electrochemical treatment. The in situ ATR-FTIR spectra were measured during the first cycle of the cyclic voltammogram for all samples.

The construction of the spectroelectrochemical cell is given in Figure 1. The polymer films were initially equilibrated in the spectroelectrochemical cell containing the supporting electrolyte solution at the starting potential of −0.5 V, and a spectrum was taken for reference. Twenty-two IR spectra were taken during one cyclic voltammogram each covering a range of about 80 mV in the potential scan. The cyclic voltammograms were measured at a scan rate of 4 mV/s.

RESULTS AND DISCUSSION

The in situ FTIR spectra and the corresponding cyclic voltammograms of the different PANI structures are given in Figure 2. The electrode potentials at which the IR spectra were measured are shown by dots on the voltammetric curve.

A first analysis of the in situ IR spectra appoints to the broad band in the region from 1800 to 7000 cm^{-1} characteristic for the intermediate oxidized metallic form of PANI. In this range, maxima can be observed around 4500−5000 cm^{-1} at electrode potentials of the conductive form of PANI, which decrease in

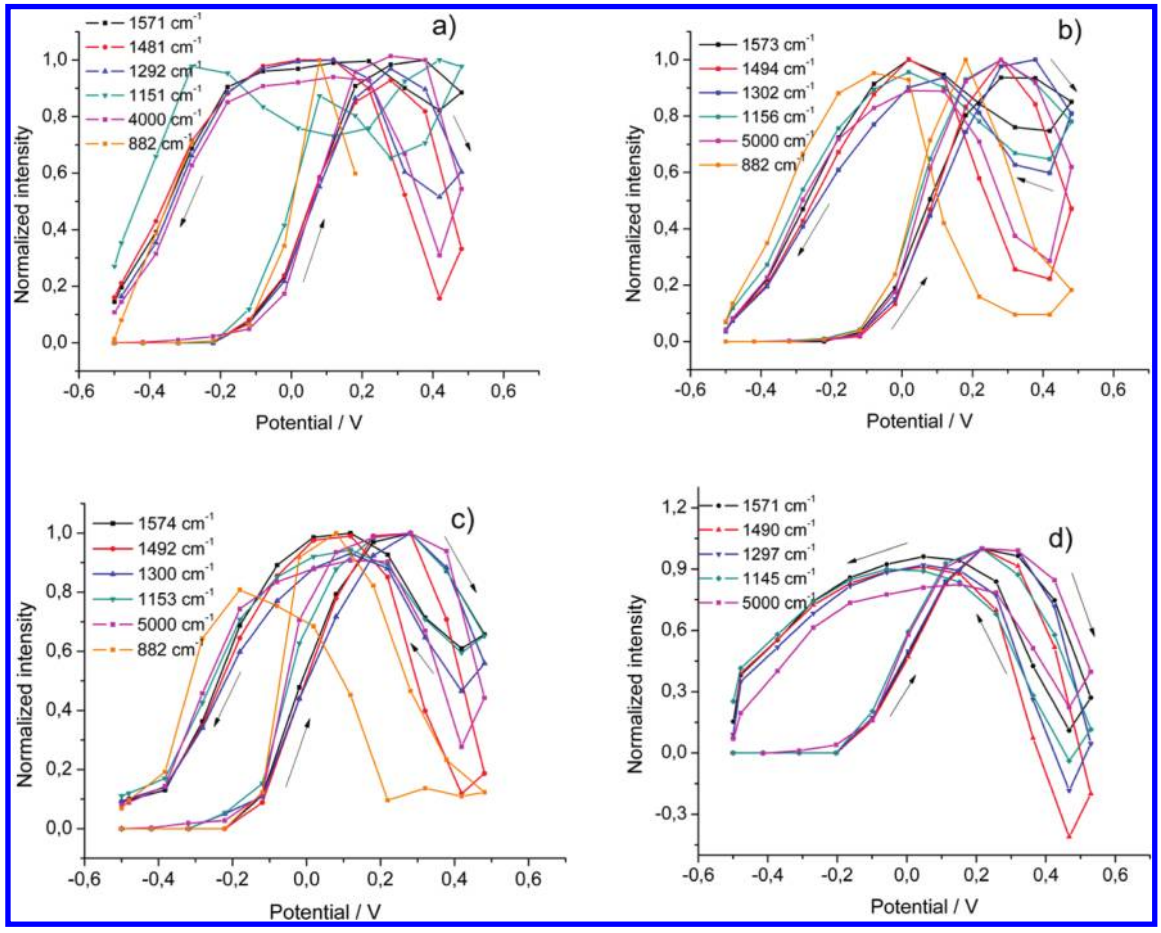

Figure 3. Potential dependence of semiquinoid bands and of the free charge carrier band for the PANI structures EB1 (a), EB2 (b), EB3 (c) and ES (d).

dx.doi.org/10.1021/jp211595n | J. Phys. Chem. B 2012, 116, 4377−4385

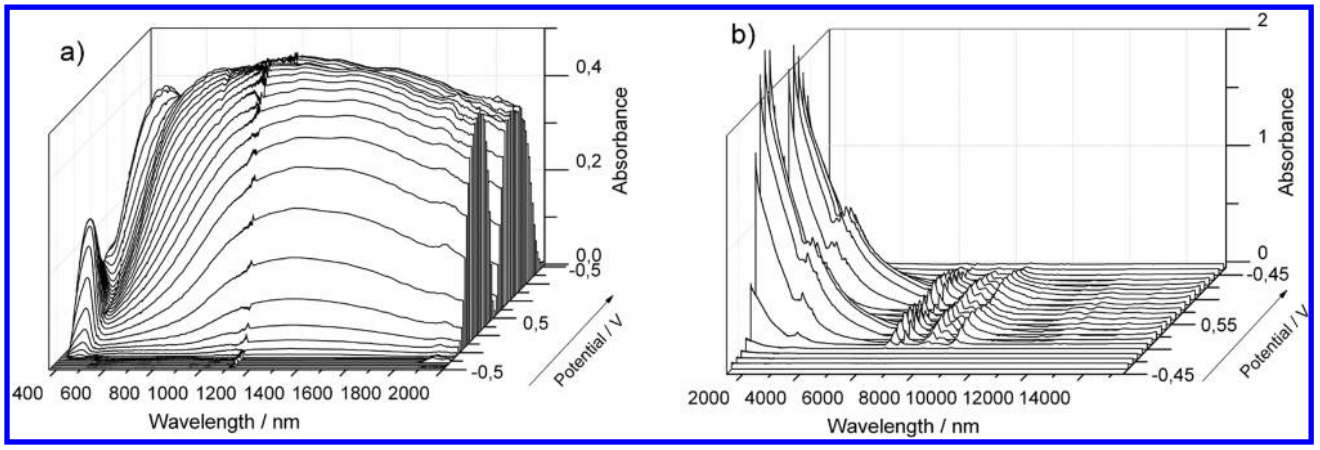

Figure 4. In situ UV−vis−NIR (a)[24] and in situ ATR-FTIR (b) spectra recorded during the oxidation/rereduction of EB2. The experimental conditions are the same in both spectroscopic techniques, except for the working electrode: indium tin oxide for UV−vis−NIR, and ZnSe-Au for FTIR measurements.

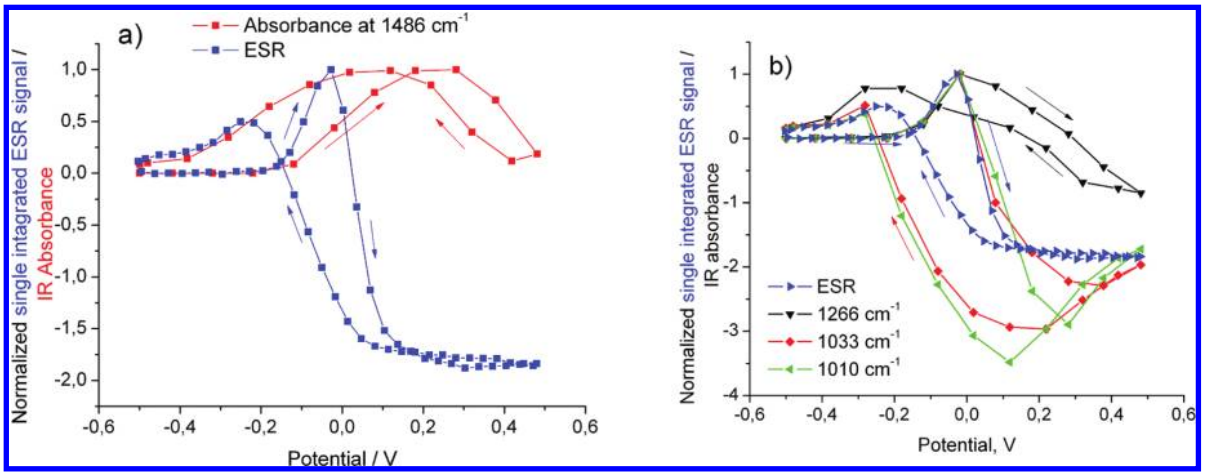

Figure 5. Potential dependence of spectroscopic data of PANI (EB3) during the oxidation/rereduction of (a) a single integrated ESR signal and one selected IR band and (b) polaronic bands at 1266, 1033, and 1010 cm^{-1}.

intensity at electrode potentials where the nonconductive form is present. The in situ FTIR spectra show some bands in the range from 3000−3300 cm^{-1} caused by N−H stretching vibrations in the polymer structure and O−H vibrations of the aqueous solution. To avoid any misinterpretations, this part of the IR spectra was not analyzed. In the mid infrared region, four major increasing peaks and four major decreasing peaks during oxidation are found. A summary of the analysis of these peaks is given in Table 1, including their assignments. The peak positions are potential dependent, i.e., the wavelength is shifting to higher/lower values during oxidation, indicating a change to quinoid structures and a reformation of the initial structure during rereduction.

Emeraldine bases as a powder give major vibrations at around 1600, 1500, 1300, 1170, and 820 cm^{-1}. The decrease of the vibration bands around 1500 and 814 cm^{-1} related to the benzene ring mode and of the band above 1200 cm^{-1} corresponding to the C−N stretching in aromatic amines are consistent with a loss of the benzoid ring structure, which is transferred into semiquinoid or quinoid ones, including the transformation of amino groups into imino groups upon oxidation of the polymer.

The potential dependence of the four major bands in mid-infrared region is the same for EB1, EB2, EB3, and ES. They start to increase at potentials around −0.22 V and reach a maximum at around 0.28 V in the forward scan. In the backward scan they increase and again reach a maximum at around 0 V as shown in Figure 3.

The potential dependence of the broad band at 5000 cm^{-1} (4000 cm^{-1} for EB1) and that of the four major bands in the mid infrared region around 1570, 1490, 1300, 1150, and 882 cm^{-1} are the same. The in situ IR spectra of all PANI structures under study show a broad band with high intensity in the mid- and near-infrared region from 1800 to 7000 cm^{-1}. Figure 4 gives a comparative presentation of in situ ultraviolet−visible−near-infrared (UV−vis−NIR)[24] and in situ ATR-FTIR spectra recorded during the oxidation/rereduction of EB2. From these two parts of the figure, it is obvious that the broad band in the IR spectra is a tail of the broad NIR band at ca. 1300 nm in the UV−vis-NIR spectra, indicating that these bands correspond to the same charged structure.

The potential dependence of the IR bands at 5000, 1570, 1490, 1300, 1150, and 882 cm^{-1} does not coincide with that of the electron spin resonance (ESR) signal (Figure 5a).[24] Therefore these bands have been attributed to the formation of a spinless doubly charged species such as π-dimers. The same behavior was found for electrochemically prepared PANI and the aniline-phenosafranine copolymers as well.[35] The IR study of PANI, phenazine polymer, and the aniline−phenazine copolymers showed that the band at ca. 880 cm^{-1} is attributed

dx.doi.org/10.1021/jp211595n | J. Phys. Chem. B 2012, 116, 4377−4385

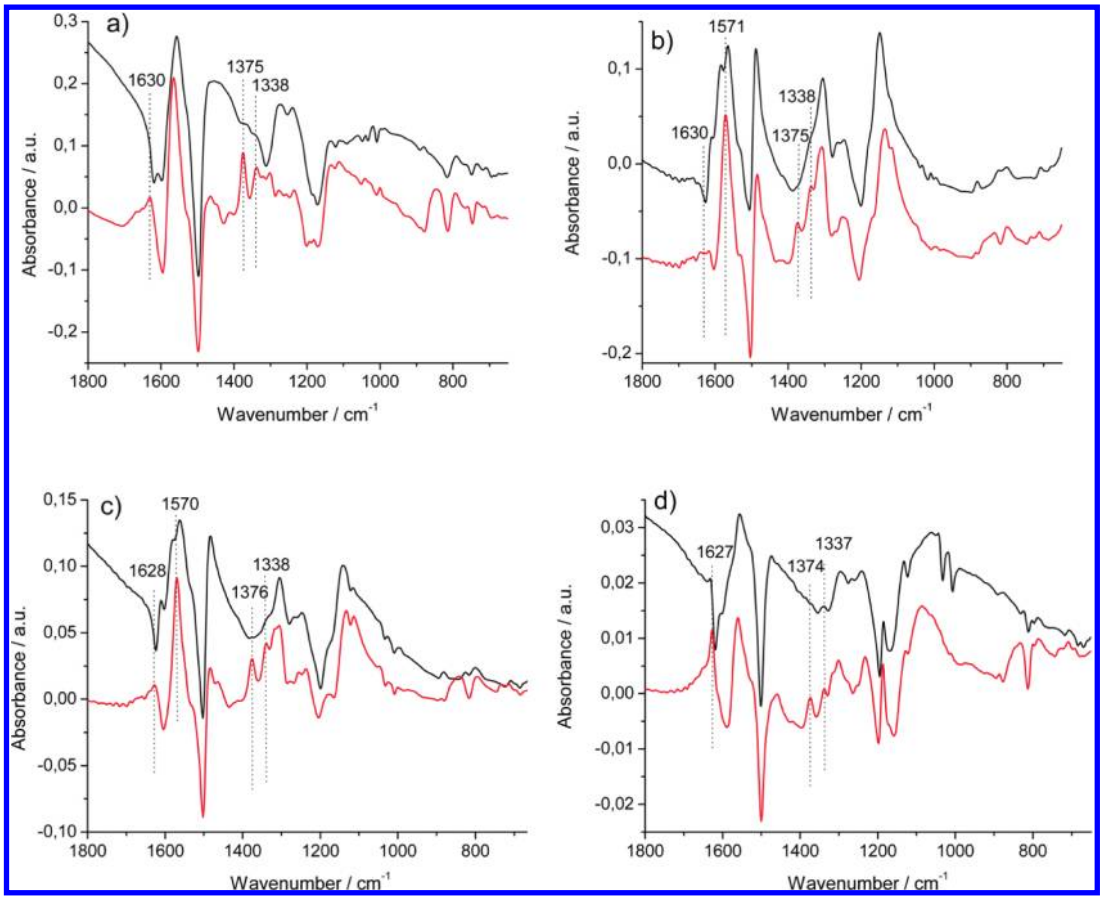

Figure 6. IR spectra of PANI structures after the first (black line) and the second redox peak (red line) in the cyclic voltammogram for (a) EB1, (b) EB2, (c) EB3, and (d) ES.

to a 2-substituted phenazine ring.[24] The same potential dependence of the bands attributed to the π-dimer and of the band at 882 cm^{-1}, which is associated with the branches in the polymer, indicates that the π-dimers are stabilized at the phenazine-like units of the polymer chain.

Together with the vibrations attributed to the π-dimers, further bands at 1266, 1033, and 1010 cm^{-1} start to rise at potentials above −0.22 V, having a similar potential dependency at low oxidation levels. A completely different potential dependency is observed at higher potentials. They increase in intensity and reach a maximum at potentials of about 0.08 V for EB2 and −0.02 V for EB3; afterward they start to decrease, even going to negative values. In the back scan they reach a maximum at around −0.28 V. The band at 1266 cm^{-1} is attributed to C−$N^{\bullet+}$ stretching in semiquinone radical cations, in agreement with Raman spectroscopic studies, which gives a band at around 1250 cm^{-1} attributed to the polaron lattice structure.[15,16] The bands at 1010 and 1033 cm^{-1} could be ascribed to the C−H in-plane deformation vibration of 1,4-disubstituted or 1,2,4-trisubstituted benzene rings. Because polarons and π-dimers have the same basic chemical structure, a differentiation of IR peaks corresponding to π-dimers and those attributed to polarons is only possible by comparing their potential dependence with that of the ESR signal. The potential dependence of these bands, given in Figure 5b, is very similar to those observed for the ESR signal;[24] therefore they are ascribed to polaronic structures.

The decrease of these bands to negative values can be explained by the fact that polarons exist in the initial state of the polymers as shown by the ESR spectra of emeraldine bases, which have a signal even in the uncharged state.[24] The potential dependence of the ESR signal is referenced to the initial state, thus starting with an ESR signal of "0" intensity and shows the differences induced by p-doping compared to the initial state. In the early stages of oxidation, an additional amount of polarons is generated. By further oxidation, a larger amount of polarons than that generated in the voltammetric scan is transformed into dicationic species, giving rise to a negative absorption band in the in situ FTIR spectra. Thus, the negative values of the IR bands during the oxidation of the polymer at higher potentials can be explained by a larger amount of polarons in the reference spectrum than in the in situ spectra upon oxidation. The difference between the ESR intensity at the initial and the reverse potential increases in the row EB1 < EB2 < EB3.[24] The obtained potential dependencies of the 1266, 1033, and 1010 cm^{-1} IR bands are in good agreement with these observations. As shown by the IR spectroscopy of emeraldine bases as a powder, the branching of the polymer structure increases with increasing weight average molecular weight of the polymer.[24] There is a correlation of the amount of polarons and the branching of the polymer chain. EB3 as the most branched polymer structure has a maximum amount of polarons in the initial state. The IR bands ascribed to polarons show a strong decrease to negative intensities in the case of EB3 due to a larger amount of polarons available from the beginning, which is further oxidized to other charged species. This fact together with the appearance of the band at 1033 cm^{-1} also demonstrates that polarons are stabilized on the

dx.doi.org/10.1021/jp211595n | J. Phys. Chem. B 2012, 116, 4377−4385

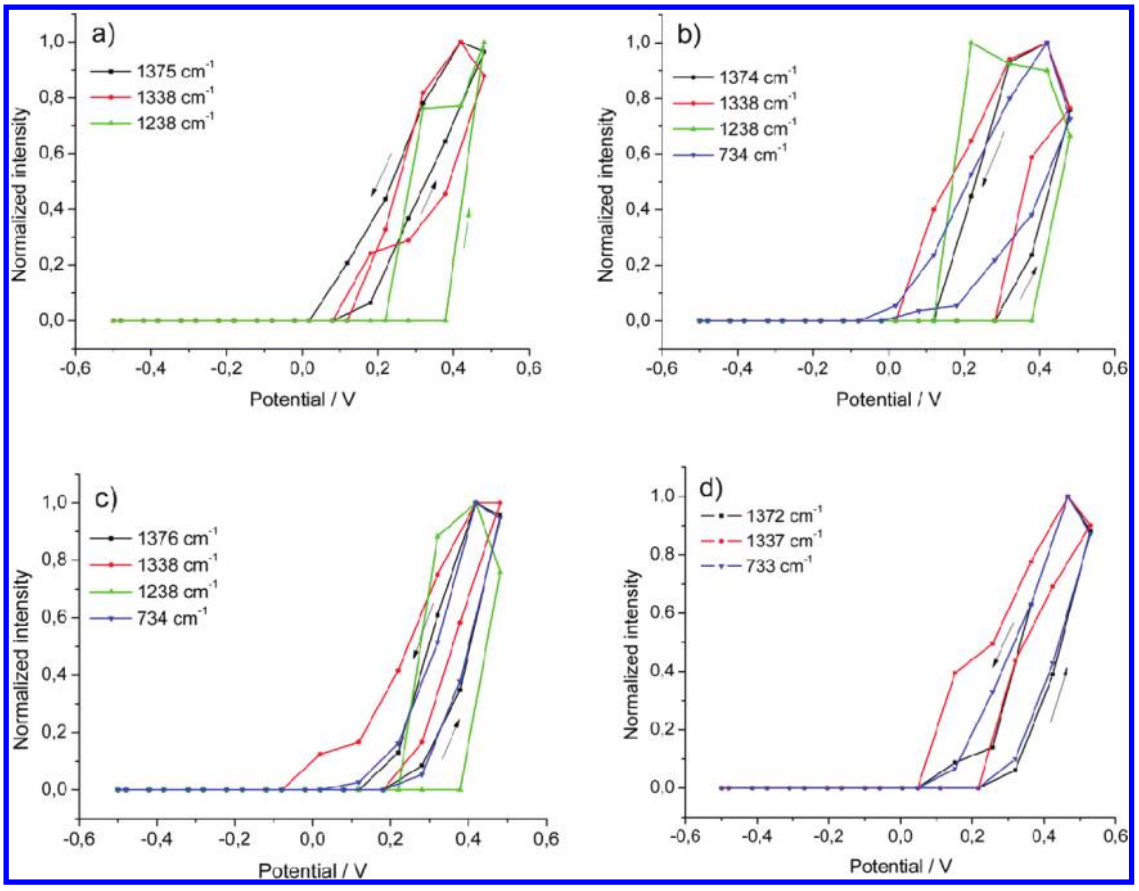

Figure 7. Potential dependence of bipolaronic bands in PANI structures: (a) EB1, (b) EB2, (c) EB3, and (d) ES.

Table 2. FTIR Bands of Bipolarons as Protonated Quinoid Structures

EB1	EB2	EB3	ES	assignment[a]
1630	1628	1627	1630	ν (C═N) in Q ring
1556	1571	1563	1553	ν (C═C) in Q ring
1372	1374	1376	1372	ν (C−N) near QBQ
1338	1338	1338	1337	ν (C−N) near QBQ
1235	1238	1236	-	ν (C−N)
734	734	734	733	δ (C−H) in Phz

[a]Assignments are based on refs 25−38. ν, stretching mode; δ, in-plane bending mode; B, benzene ring; Q, quinoid ring; Phz, phenazine.

linear polymer segments close to the branches by phenazine-like units in the polymer chains.

At higher electrode potential, where the polaronic bands start to decrease, new bands are arising at 1630, 1238, 1375, and 1338 cm^{-1} in the in situ FTIR spectra. The band at 1630 cm^{-1} is assigned to the C═N stretching in quinoid rings, the bands at 1375 and 1338 cm^{-1} to C−N stretching in the neighborhood of quinoid rings. The evolution of these new bands can be evidenced by comparing the in situ FTIR spectra after the first and second oxidation peaks, as shown in Figure 6. These bands are observed during the second redox peak in the cyclic voltammogram and correspond to the formation of bipolarons as protonated quinoid structures.

The IR bands at 1375 and 1338 cm^{-1} start to increase at electrode potentials around 0.18 V for EB1, 0.38 V for EB2, and 0.28 V for EB3 and ES. They all reach a maximum at the reversal potential and completely disappear at around 0.02 V. This potential dependence is opposite to that of bands assigned

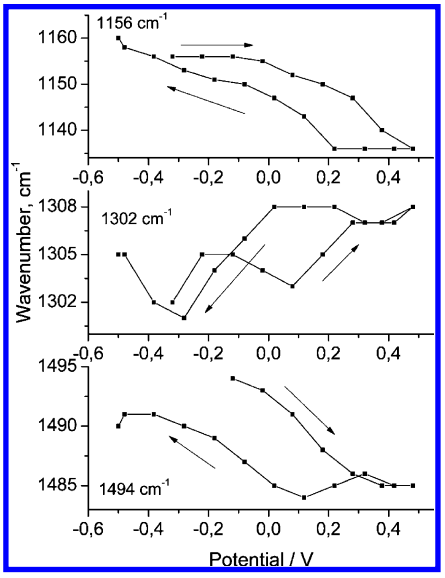

Figure 8. Shift of initial IR bands at 1494, 1302, and 1156 cm^{-1} during the oxidation and rereduction of PANI structure EB2.

to π-dimers. The π-dimer bands start to decrease above potentials of 0.28 V where the bipolaronic bands start to increase and reach a maximum at 0 V in the back scan, where the bipolaronic bands completely disappear. This could be interpreted assuming a reaction scheme where π-dimers are transformed to bipolarons at higher oxidation levels. The potential dependence of these new bands is given in Figure 7, and a summary of the bipolaronic bands is given in Table 2.

dx.doi.org/10.1021/jp211595n | J. Phys. Chem. B 2012, 116, 4377−4385

Evidence for the formation of quinoid rings during the oxidation can also be found by the shift of the IR band positions attributed to semiquinoid structures as shown in Figure 8.

The IR bands at 1494 and 1156 cm^{-1} are shifted to lower wavenumbers, and the band at 1302 cm^{-1} is shifted to higher wavenumbers, which corresponds to a similar shift observed in leucoemeraldine, emeraldine, and pernigraniline base.[25]

The main IR band around 1570 cm^{-1} starts at 1573 cm^{-1} accompanied by a shoulder at 1590 cm^{-1}. Both bands are increasing with potential and shift to lower wavenumbers. At high electrode potentials, only one new band at 1570 cm^{-1} dominates the IR spectra, corresponding to a pure quinoid structure.

The combination of in situ ESR/UV−vis−NIR and in situ ATR-FTIR spectroelectrochemistry confirms the mechanism of electrode reactions, which was proposed in our earlier work.[35] Figure 9 gives the scheme for the formation of charged states

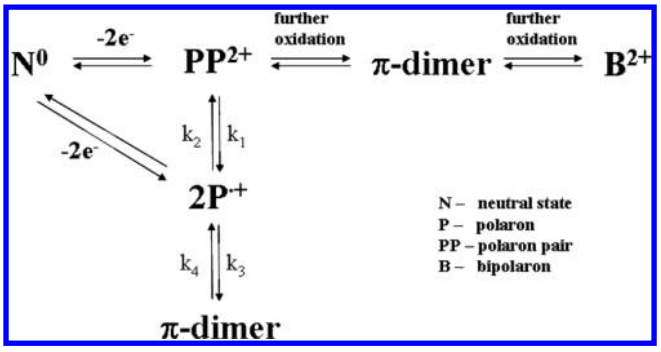

Figure 9. Scheme for formation of charged states upon electrochemical oxidation of PANI.

upon p-doping of PANI. At the early stage of charge injection into the polymer, a polaron pair is formed. Polarons and π-dimers are formed at the same potential. At that potential where the concentration of π-dimers is at its maximum, no ESR signal is observed. This behavior points to the fact that the polarons are converted into π-dimers at higher oxidation levels. The further p-doping of the PANI leads to the transfer of π-dimers into bipolarons.

CONCLUSIONS

By in situ FTIR spectroelectrochemistry, the formation of charged states (polarons, bipolarons, π-dimers) in PANI during its p-doping was studied in detail. The potential dependence of the IR bands is used to follow the formation of charged species in its potential dependence.

The broad IR band in the region 7000−1700 cm^{-1} in the in situ spectra is a tail of the broad absorption band at 1300 nm found in the in situ UV−vis−NIR spectra. The IR bands at 5000, 1570, 1490, 1300, and 1150 cm^{-1} have the same potential dependence and dominate the IR spectra. They are attributed to the semiquinoid structure of the polymer. The comparative analysis of the potential dependence of these IR bands with that of ESR signal found in our earlier studies showed that they can be associated with a π-dimer formed by two polarons. A band at 882 cm^{-1} corresponding to a substituted phenazine ring and having a similar potential dependency as those of semiquinoid bands demonstrates that π-dimers are stabilized near the phenazine units.

The IR bands at 1266, 1033, and 1010 cm^{-1} were attributed to the polaronic structure in the polymer because their potential dependencies coincide with that of the ESR signal. The appearance of a band at 1033 cm^{-1} attributed to the branched polymer structure demonstrates that polarons are stabilized on the linear segments at the branches in the polymer chains.

The IR bands observed at 1375, 1338, 1238, and 734 cm^{-1} during the second redox peak correspond to the formation of bipolarons. The band at 734 cm^{-1} attributed to the C−H out-of plane deformation in phenazine ring indicates that bipolarons are also stabilized near the phenazine units.

The three different potential dependencies of the IR bands found for EB1, EB2, EB3, and ES are ascribed to the formation of π-dimers, polarons, and bipolarons. The potential dependence of the spectroscopic data confirmed the mechanism of formation of charged states upon electrochemical oxidation of PANI proposed earlier.

AUTHOR INFORMATION

Corresponding Author

*E-mail: andrea.kellenberger@chim.upt.ro; Fax: +40 256 40 3060; Tel: +40 256 40 4178 (A.K.). E-mail: l.dunsch@ifw-dresden.de; Fax: +49 351 4659 811; Tel: +49 351 4659 660 (L.D.).

Notes

The authors declare no competing financial interest.

ACKNOWLEDGMENTS

The financial support offered by the BMBF is gratefully acknowledged. A.K. is thankful for the financial support of IFW Dresden. We thank Dr. I. Mönch and co-workers (IFW Dresden) for preparing the gold coatings on the ATR crystal and F. Ziegs and M. Rosenkranz (all of IFW Dresden) for discussions and technical support.

REFERENCES

(1) MacDiarmid, A. G. *Angew. Chem., Int. Ed.* **2001**, *40*, 2581−2590.
(2) Huang, W.-S.; Humphrey, B. D.; MacDiarmid, A. G. *J. Chem. Soc., Faraday Trans.* **1986**, *82*, 2385−2400.
(3) Brédas, J. L.; Scot, J. C.; Yakushi, K.; Street, G. B. *Phys. Rev. B* **1984**, *30*, 1023−1025.
(4) Fesser, K.; Bishop, A. R.; Campbell, D. K. *Phys. Rev. B* **1983**, *27*, 4804−4825.
(5) [(a) Hill, M. G.; Mann, K. R.; Miller, L. L.; Penneau, J. F. *J. Am. Chem. Soc.* **1992**, *114*, 2728−2730. (b) Miller, L. L.; Mann, K. R. *Acc. Chem. Res.* **1996**, *29*, 417−423.
(6) Vorotyntsev, M. A.; Heinze, J. *Electrochim. Acta* **2001**, *46*, 3309−3324.
(7) (a) Nekrasov, A. A.; Ivanov, V. F.; Gribkova, O. L.; Vannikov, A. V. *Russ. J. Electrochem* **2004**, *40*, 249−258. (b) Nekrasov, A. A.; Ivanov, V. F.; Gribkova, O. L.; Vannikov, A. V. *Electrochim. Acta* **2005**, *50*, 1605−1613. (c) Gospodinova, N.; Dorey, S.; Ivanova, A.; Zhekova, H.; Tadjer, A. *Int. J. Polym. Anal. Charact.* **2007**, *12*, 251−271.
(8) Petr, A.; Wei, D.; Kvarnström, C.; Ivaska, A.; Dunsch, L. *J. Phys. Chem. B* **2007**, *111*, 12395−12398.
(9) Kvarnström, C.; Ivaska, A.; Neugebauer, H. *Advanced Functional Molecules and Polymers*; Nalwa, H.S., Ed.; Gordon and Breach Science: New York, 2001; Vol. *2*, Chapter 6, pp 139−170.
(10) Sturm, J.; Künzelmann, U.; Bischoff, S.; Dunsch, L. *Bruker Report No. 142*, 1996, pp 8−11.
(11) Zimmermann, A.; Künzelmann, U.; Dunsch, L. *Synth. Met.* **1998**, *93*, 17−25.
(12) Ping, Z.; Neugebauer, H.; Neckel, A. *Electrochim. Acta* **1996**, *41*, 767−772.
(13) Ping, Z.; Nauer, G. E.; Neugebauer, H.; Theiner, J.; Neckel, A. *J. Chem. Soc., Faraday Trans.* **1997**, *93*, 121−129.

(14) Šeděnková, I.; Trchová, M.; Blinova, N.; Stejskal, J. *Thin Solid Films* **2006**, *515*, 1640−1646.
(15) Quillard, S.; Louarn, G.; Buisson, J. P.; Boyer, M.; Lapkowski, M.; Pron, A.; Lefrant, S. *Synth. Met.* **1997**, *84*, 805−806.
(16) Furukawa, Y.; Ueda, F.; Hyodo, Y.; Harada, I.; Nakajima, T.; Kawagoe, T. *Macromolecules* **1988**, *21*, 1297−1305.
(17) Sariciftci, N. S.; Kuzmany, H.; Neugebauer, H.; Neckel, A. *J. Chem. Phys.* **1990**, *92*, 4530−4539.
(18) Xia, Y.; Wiesinger, J. M.; MacDiarmid, A. G.; Epstein, A. *Chem. Mater.* **1995**, *7*, 443−445.
(19) Willstätter, R.; Moore, C. W. *Ber. Dtsch. Chem. Ges.* **1907**, *40*, 2665−2689.
(20) Green, A. G.; Woodhead, A. E. *Ber. Dtsch. Chem. Ges.* **1913**, *46*, 33−49.
(21) Dunsch, L. Dissertation, Bergakademie Freiberg, Germany, 1973.
(22) Trchová, M.; Šeděnková, I.; Konyushenko, E. N.; Stejskal, J.; Holler, P.; Ćirić-Marjanović, G. *J. Phys. Chem. B* **2006**, *110*, 9461−9468.
(23) Do Nascimento, G. M.; Temperini, M. L. A. *J. Raman Spectrosc.* **2008**, *39*, 772−778.
(24) Dmitrieva, E.; Dunsch, L. *J. Phys. Chem. B* **2011**, *115*, 6401−6411.
(25) Quillard, S.; Louarn, G.; Lefrant, S.; Macdiarmid, A. G. *Phys. Rev. B* **1994**, *50*, 12496−12508.
(26) Louarn, G.; Lapkowski, M.; Quillard, S.; Pron, A.; Buisson, J. P.; Lefrant, S. *J. Phys. Chem.* **1996**, *100*, 6998−7006.
(27) Boyer, M. I.; Quillard, S.; Louarn, G.; Froyer, G.; Lefrant, S. *J. Phys. Chem. B* **2000**, *104*, 8952−8961.
(28) Socrates, G. *Infrared and Raman Characteristic Group Frequencies. Table and Charts*, 3rd ed; John Wiley and Sons: Chichester, U.K., 2001; pp 107−113, 123, 157−167, 176−177, 220−222.
(29) Tang, J.; Jing, X.; Wang, B.; Wang, F. *Synth. Met.* **1988**, *24*, 231−238.
(30) Ping, Z. *J. Chem. Soc., Faraday Trans.* **1996**, *92*, 3063−3067.
(31) Zimmermann, A.; Dunsch, L. *J. Mol. Struct.* **1997**, *410*−*411*, 165−171.
(32) Trchová, M.; Šeděnková, I.; Tobolková, E.; Stejskal, J. *Polym. Degrad. Stab.* **2004**, *86*, 179−185.
(33) Trchová, M.; Stejskal, J.; Prokeš, J. *Synth. Met.* **1999**, *101*, 840−841.
(34) Trchová, M.; Šeděnková, I.; Stejskal, J. *Synth. Met.* **2005**, *154*, 1−4.
(35) Kellenberger, A.; Dmitrieva, E.; Dunsch, L. *Phys. Chem. Chem. Phys.* **2011**, *13*, 3411−3420.
(36) Stammer, C.; Taurins, A. *Spectrochim. Acta* **1963**, *19*, 1625−1653.
(37) Li, X.-G.; Huang, M.-R.; Duan, W.; Yang, Y.-L. *Chem. Rev.* **2002**, *102*, 2925−3030.
(38) Chen, C.; Gao, Y. *Electrochim. Acta* **2007**, *52*, 3143−3148.